Est. 1984

ORIENTAL JOURNAL OF CHEMISTRY
An International Open Access, Peer Reviewed Research Journal

www.orientjchem.org

ISSN: 0970-020 X
CODEN: OJCHEG
2023, Vol. 39, No.(4):
Pg. 963-969

Effect of Ag ion Implantation on the Crystallinity and Optical Property of Spin-coated TiO_2 thin Films

SUNIL KUMAR[1]*, HANSRAJ SHARMA[1], JAGDISH PARSAD[2], JAGAVENDRA YADAV[1] and MANGEJ SINGH[1]

[1]Department of Physics, University of Rajasthan, Jaipur, India.
*Corresponding author E-mail: sunilnehra161196@gmail.com

http://dx.doi.org/10.13005/ojc/390419

(Received: July 11, 2023; Accepted: August 12, 2023)

ABSTRACT

By using the spin coating method, Ag ion implanted TiO_2 layers were deposited. These thin films were made on a glass substrate that had been meticulously cleaned. The characterization of synthesized Ag-dopped TiO_2 thin films by XRD, UV-Vis spectrometer, and SEM with EDX. The outcomes demonstrated the presence of crystalline anatase phase and smooth surface morphologies in the Ag-TiO_2 films that were annealed at 500^{0}C. SEM results are utilized to investigate the surface morphology and element identification that has been verified by EDX analysis. The band gap for undoped TiO_2 and silver-dopped TiO_2 thin films is suggested by the UV-Vis investigation and we get it 2.88eV, 2.96eV, and 3.16eV subsequently. In addition, the findings showed that compared to undoped TiO_2 films, the Ag-doped TiO_2 film demonstrated higher photocatalytic activity.

Keywords: Titanium oxide, Silver doped titanium dioxide, Sol-gel procedure, X-ray diffraction, Snnealing temperature.

INTRODUCTION

Metal oxide-based semiconductors are classified as a key class of substance because of their extraordinary basic mechanical, chemical, electrical, optical, and luminous capabilities[1,2]. The ability of nanosized TiO_2 to act as a photocatalyst was initially identified in 1967 by Akira Fuji Shima, who then published his findings in 1972[3]. This is primarily a result of its advantageous characteristics, such as non-toxicity, molecular inertness, and persistence across a broad range of pH values under illumination circumstances[4]. TiO_2, a semiconductor material, is utilized in a few processes, according to studies, TiO_2 can be utilized in many different applications, such as dielectric layers, solar cells, self-cleaning windows, biohybrid interfaces lithium batteries, optoelectronics devices, gas detection, and air-water purification[5-11].

Due to present environmental issues, TiO_2 has emerged as the prime popular semiconductor for heterogenous photocatalysis and has generated significant interest from scientists. Anatase-rutile-brookite are the three phases of TiO_2 crystallization that are most often known. As a phase, rutile is the most stable although anatase is the most active.

With the help of UV-light (wavelength of 380nm), the anatase band gap (E_g>3.22eV) is activated, permitting electrons to move from the valence band to the conduction region[12]. As an outcome, photocatalytic reactions on TiO_2 are constrained in their use of visible light as an excitation source[13].

The photons absorption on the surface to produce electron-hole pairs is one of the photocatalytic reaction's most significant characteristics. The shape of the films, which affects their photocatalytic activities, significantly impacts this pair's production[14-15]. By altering the surface of semiconductor particles, the electron transport efficacy may be increased. Numerous techniques, such as the incorporation of TiO_2 with noble metal ions and transition metal ions as well as the addition of nonmetal ions (C, B, S, F, Cl)[16-19], connected semiconductors systems[20], dye sensitization[21], can be used to alter the surface of the semiconductor. It was discovered that native metals including silver, gold, platinum, and palladium, when coated on a TiO_2 surface, improve the photocatalytic efficiencies in a variety of ways, including by trapping electrons and preventing the reunify of Ele-hole pairs and improving the e/h pairs[22-23]. Additionally, noble metals were shown to enhance visible light absorption, enabling surface electron activation by plasmon resonances[24]. The alteration of the photocatalyst surface's characteristic is another result of the noble metal addition[25].

Ag metal doping of TiO_2 thin films has got a lot of focus since it has so many intriguing qualities, such as outstanding effectiveness, relatively inexpensive in comparison to other noble metals, antibacterial capabilities[26], and strong oxygen binding response[27].

The preparation procedure has a substantial influence on all physical attributes and photocatalytic activity of thin films. Several techniques for preparing TiO_2 thin films have been developed during the last two decades, including atmospheric pressure chemical vapor deposition (CVD)[28], sputtering[29], electron beam evaporation[30], and sol-gel approach[31].

The sol-gel spin-coating method is the best choice for creating vitreous or multilayer films on a range of substrates when excellent consistency, pureness, and homogeneity are required.

The main objective of the study was to develop silver-doped TiO_2 (phase-anatase) opaque thin films backed by glass substrate by applying the sol-gel process. In addition, the impact of silver ions on the evolution of the crystalline structure, the mechanism of grain growth, and the characteristics of the optical and photocatalytic activity prior to and subsequent to surface enhancement with metallic silver were investigated as well.

MATERIALS AND METHODS

Chemicals

TTIP [$Ti(O\text{-}i\text{-}C_3H_7)_4$], ethanol ($CH_3CH_2OH$), DI water, and HCl (Hydrochloric acid) all materials purchased from CDH Private Limited, Delhi. All the materials are AR grade, which is used to prepare TiO_2 sol.

Cleanup of Substrates

We cleaned substrates made of glass in isopropanol, Deionized water (DI), and acetone for a total of 30 minutes. The Glass substrates were lastly stored in Deionized water (DI water) before use.

Thin films deposition

For undoped thin films of TiO_2 First, we combine 0.1 Mol of TTIP [$Ti(O\text{-}i\text{-}C_3H_7)_4$] and 25 mL of ethanol ($CH_3CH_2OH$) in a beaker. 2.30 h were used for stirring at fifty degrees Celsius. In order to lessen evaporation, the precursor solution was covered with an aluminum sheet carefully. Following that, remove the aluminum sheet and add 2 g ethyl-cellulose (as a binder) and continue stirring. After that, a solution consisting of 25 mL of ethanol, 0.1 mol of HCL, and 0.1 mol of DI water was added by dropper and stirred for 36 h at 50°C. then we obtained a light yellowish TiO_2 solution.

For doped thin films, a solution containing 25 mL of ethanol, 0.1 mol of HCl, 0.1 mol of DI water, and silver nitrate ($AgNO_3$- according to doping) was added and stirred for 36 h at 50°C. Then a light white TiO_2 solution was sent to us.

The resulting mixture was then spin-coated at 1800rpm for 25 sec. onto a non-conducting glass substrate. To eliminate the solvents and other impurities, the deposited TiO_2 thin films were heated to 110°C and baked for 3 minutes. After that, the baked film was heated for 90 min at 45°C.

Characterization Techniques

The X-ray Diffraction technology "Panalytical X Pert Pro" using CuK radiation technology with CuK radiation was performed to figure out the crystal framework of pure, Ag ion implanted TiO_2 thin films at the surrounding temperature. Scherrer's equation is used to calculate the crystal size.

Using the Nova Nano SEM 450 and "scanning electron microscopy", the surface morphology was studied. AFM using a Multimode Scanning Probe Microscope (Bruker) was used to examine the surface topography.

Spin-coated pure and Ag-implanted films served as samples and standards, and the spectral absorbance of TiO_2 thin films was figured out using a LAMBDA-750 (version name) UV-Vis-NIR Spectrophotometer.

RESULTS AND DISCUSSION

XR-D approach-Structural examination

To explore the structure of crystalline materials, XRD, a trustworthy and widely used identification method, is applied[32]. After the analysis of the XRD data, plot a graph of undoped, 1% Ag-implanted and 2% Ag-implanted TiO_2 thin films were shown in Fig. 1a. Anatase is the most known phase of TiO_2. The indices of the phases are listed in parenthesis and denoted by the letter "A". These patterns clearly show that for an undoped TiO_2 thin film, the diffraction peak is observed at 2=25.430, which corresponds to the diffraction plane with Miller indices (101). While all of these peaks are associated with TiO_2's anatase phase. By correlating these spikes with PDF cards #00-21-1272 and #00-21-1276, respectively, it was determined that the tetragonal anatase phase had formed. As a result, with a minor contribution from the rutile phase, these thin films largely frame out in the anatase phase. The fact that when 1% and 2% Ag were incorporated into TiO_2 thin film, neither a new peak nor a change in peak position was created proved the stability of the anatase and rutile phases upon Ag doping. Instead of forming a chemical link with the Ag atoms in the TiO_2 matrix, the Ag atoms simply exist there in nanoclusters[33,34].

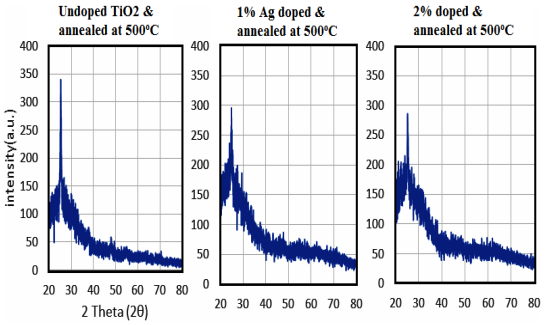

Fig. 1(a). XR-D plot of the pure, 1(b) 1% Ag doped & 1(c) 2% Ag implanted TiO_2 thin films

The lattice parameters of the tetragonal phase were derived utilizing the following calculation[35].

$$\frac{1}{d^2} = \frac{h^2 + k^2}{a^2} + \frac{l^2}{c^2}$$

The lattice parameters, in this case, are a and c, the interplanar pitch is d, and the miller indices are (hkl).

Lattice constant measurements for undoped TiO_2 are determined to be a=3.7412 and c=9.4676. The creation of the tetragonal phase of TiO_2 was validated by such features because they matched previously published literature [PDF cards #00-21-1272 and #00-21-1276]. By adding 1% & 2% Ag to TiO_2, the lattice parameters marginally grew (a=3.74, c=9.52), which is consistent according to the diffracted hikes relocating down to the lower 2 values.

Scherer's formula was employed to calculate the crystallite size[36,37].

$$D = \frac{k\lambda}{\beta \cos\theta}$$

Where K is the form component, with a magnitude of 0.9 λ, is the CuK radiation's wavelength, 1.55, and β is full width at half maxima. In contrast, θ provides the diffraction angle.

The size of the crystallite was measured by employing the biggest intensity XRD peak (XRD spike-101). Undoped TiO_2 is found to have crystallite sizes of 35.3nm, which are reduced to 33.03nm and 33.96nm when doped with 1% and 2% Ag, respectively.

Due to the deformation of the lattice and keeping in mind that the rutile phase in addition to the anatase phase of TiO_2, the size of the crystallites has diminished.

Optical properties

The UV-Vis transmittance plot of Ag-implanted TiO_2 nanocomposite thin films is displayed in Fig. 2. In the 400nm to 900nm wavelength range, Ag-doped TiO_2 films have transmittances of more than 50%. Both the transmission and reflectance spectra's wavy characteristics in the 800-400nm range are caused by the interference factor, and a rapid decline in transmittance may be connected to the excitonic transition. It is clear from the somewhat undulating transmittance curve that the Ag-implanted TiO_2 sheets are homogeneous and thin. The behavior of Ag-implanted TiO_2 films in terms of transmittance declined as the silver concentration rose, the wavelength of the films' intake edge migrated towards longer wavelengths and the peak's intensity has grown[38,39]. Based on the local surface plasmonic response (LSPR) effect, this type of change can be understood[40]. It is a result of the addition of silver. The gap between the energy level of Ag-doped TiO_2 should be less than TiO_2's (3.2eV/3.1eV).

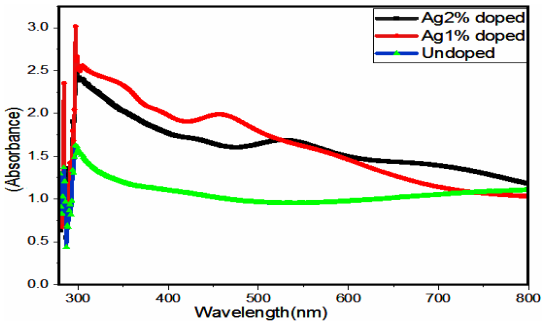

Fig. 2. UV-Visible absorption plot of pure and Ag-implanted TiO_2 thin films

Band-gap

The energy difference between the valance and conduction band (E_g) is studied using the Tauc formula. The energy axis is linearly met by extrapolating $(hv)^{1/2}$ v/s hv. The gap energy value is determined by this energy plot. The plot of $(hv)^{1/2}$ v/s hv is shown in Fig. 3. Thin films of undoped TiO_2, 1% Ag, and 2% Ag doped-TiO_2 have corresponding band gaps of 3.16 eV, 2.96eV, and 2.88ev. The band-gap energy is varying between 3.2eV and 2.8 eV as a result of Ag doping into TiO_2. The appearance of lattice distortion brought on by silver doping, which generated fresh levels of energy levels inside the TiO_2 thin film's forbidden band, is the potential cause of this band gap reduction[41]. The development of metal groupings, which resulted in regional energy levels and surface absorption, was another factor in the band gap's reduction[42].

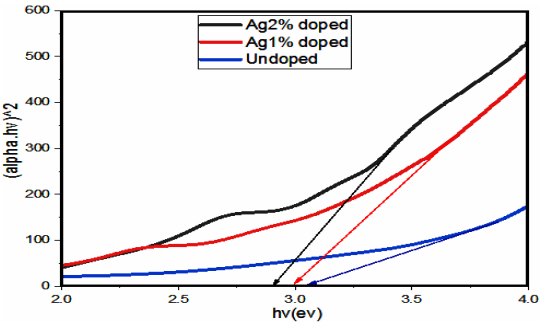

Fig. 3. Band-gap plot for undoped and Ag-implanted TiO_2 thin films

SEM Analysis

pure and silver-implanted TiO_2 films grown by the sol-gel technique on Si substrates are depicted in SEM images in Fig. 4. The type of Ag incorporation (doping) into TiO_2 film may be identified using excellent quality SEM imaging and EDX examination. SEM pictures indicate dense clusters of nano craters with sizes between 60 and 170nm. In excellent quality SEM imaging, the particular nanoparticle dispersion both inside and around the nano fissures is visible (Figrue 5).

Ag-nano-dots are nanoparticles that are around 30nm in size when they are isolated, but they can aggregate to produce particles that are 200nm in size. According to some research, increasing the Ag content may enhance the propensity to produce Ag-agglomerates.

There are no traces of the Ag component seen in the Silver doped TiO_2 films' EDX spectra (Fig. 5c). This was allocated to the increased dispersion of silver nanoparticles on the top area of the film, which limited EDX observation. The detected signal of underneath silver nanoparticles is in fact too tiny to be separated from the background signal when employing the standard acceleration voltages of 5 keV to 20 keV.

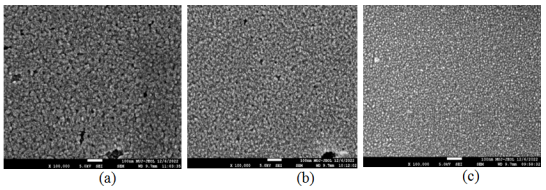

Fig. 4. SEM pictures showing the surface morphologies of undoped TiO_2 film(a), 1% Ag-doped (b), and 2% Ag-implanted TiO2 film (c)

Element	Weight%	Atomic%	Error%
OK	50.7	68.1	10.2
SiK	30.9	23.7	4.4
TiK	18.4	8.3	2.9

Element	Weight%	Atomic%	Error%
OK	51.0	66.4	9.4
SiK	40.9	30.2	3.9
Agk	0.8	0.3	8.9
TiK	7.3	3.2	5

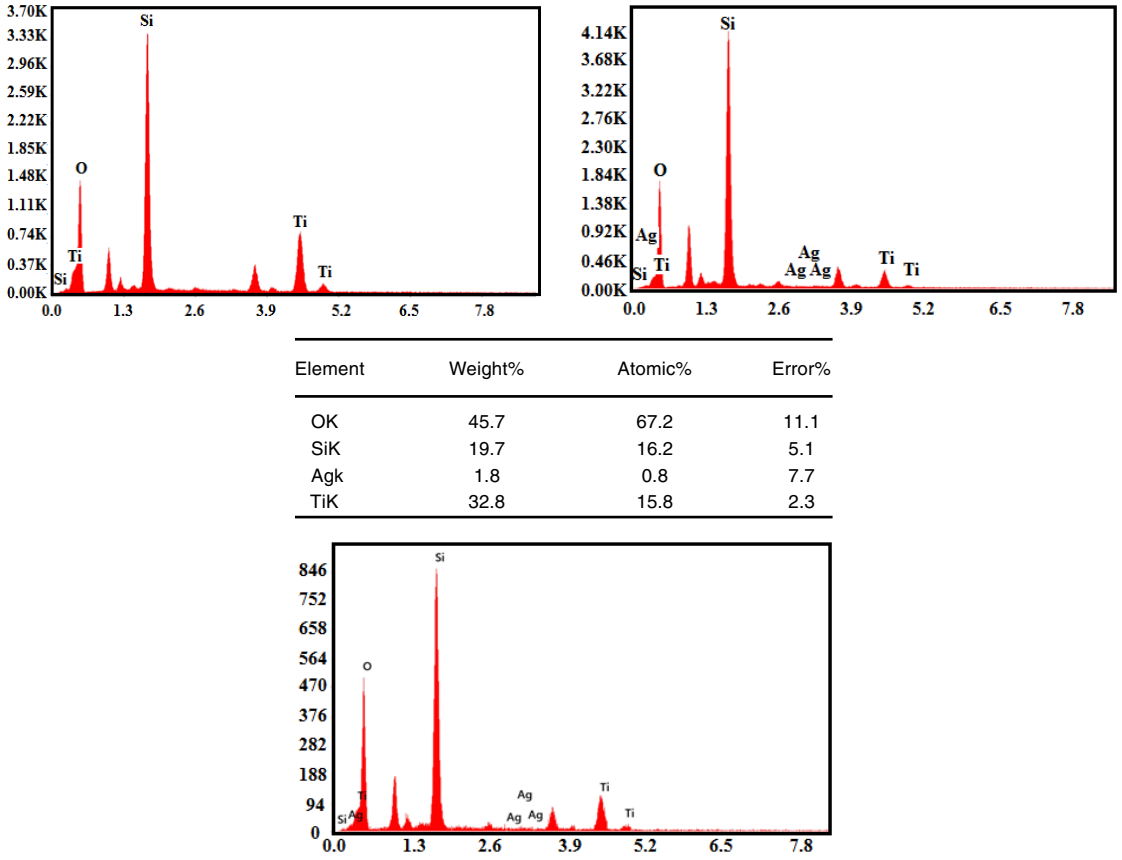

Element	Weight%	Atomic%	Error%
OK	45.7	67.2	11.1
SiK	19.7	16.2	5.1
Agk	1.8	0.8	7.7
TiK	32.8	15.8	2.3

Fig. 5. EDX plot of pure and Ag-doped TiO_2

CONCLUSION

The relatively low-cost sol-gel method has been used to create thin films of Ag-doped TiO_2 at a heating temperature of 500°C.

In comparison to pure TiO_2 films, Ag-doped TiO_2 films have smaller crystallite domain sizes.

According to X-ray diffractograms, TiO_2 developed into the anatase phases, whose lattice parameters initially grew up with Ag doping and then decreased when the fluence value was further raised.

Compared to undoped TiO_2 films, Ag-doped TiO_2 films have a greater photocatalytic function. The Eg is decreased with doping.

ACKNOWLEDGMENT

We received funding for this study from the CSIR in New Delhi, and characterization resources came from the MNIT MRC and Manipal University in Jaipur. We appreciate the facilities for experimentation and characterization provided by USIC and the physics department at UOR, Jaipur.

Conflict of interest

The authors declare that they have no known competing financial interests or personal relationships that could have appeared to influence the work reported in this article.

REFERENCES

1. Canas -Carrell J.; Metal oxide nanomaterials: health and environmental effects, *Health and Environmental Safety of Nanomaterials* (Elsevier, Amsterdam, **2014**), 200–221.
2. Kumar S.; Metal oxides for energy applications, *Colloidal Metal Oxide Nanoparticles* (Elsevier, Amsterdam, **2020**), 471–504.
3. Fujishima A.; Honda K.; Electrochemical photolysis of water at a semiconductor electrode. *Nature.,* **1972**, *238*(5358), 37–38.
4. Huang L.; Sun C.; Liu Y. Pt/N-codoped TiO_2 nanotubes and its photocatalytic activity under visible light. *Appl Surf Sci.*, **2007**, *253*(17), 7029-7035.
5. Alexandrov P.; Koprinarova J.; Todorov D.; Dielectric properties of TiO_2-films reactively sputtered from Ti in an RF magnetron, *Vacuum.*, **1996**, *47*(11), 1333-1336.
6. Dong Y. X.; Wang X. L.; Jin E. M.; Jeong S. M.; Jin B.; Lee S. H.; One-step hydrothermal synthesis of Ag decorated TiO_2 nanoparticles for dye-sensitized solar cell application, *Renewable Energy.*, **2019**, *135*, 1207-1212.
7. Choi T.; Kim J. S.; Kim J. H.; Transparent nitrogen doped TiO_2/WO_3 composite films for self-cleaning glass applications with improved photodegradation activity, *Advanced Powder Technology.*, **2016**, *27*(2), 347-353.
8. Wang J.; Wang Z.; Wang W.; Wang Y.; Hu X.; Liu J.; Gong X.; Miao W.; Ding L.; Li X and Tang J.; Synthesis, modification and application of titanium dioxide nanoparticles: A-Review, *Royal society of chemistry, Nanoscale*, **2022**, *14*, 6709-6734.
9. Javed H. M. S.; Adnan M.; Qureshi A.A.; Javed S., M.; Akram M.A.; Shahid M.; Ahmad M.I.; Afzaal M.; Abd-Rabboh H.S.M.; Arif M.; Morphological, structural, thermal and optical properties of Zn/Mg-doped TiO_2 nanostructures for optoelectronic applications, *Optics & Laser Technology.*, **2022**, *146*, 107566.
10. Ramesan M. T.; Santhi V.; Bahuleyan B. K.; Al-Maghrabi M.A.; Structural characterization, material properties and sensor application study of in situ polymerized polypyrrole/silver doped titanium dioxide nanocomposites, *Materials Chemistry and Physics.*, **2018**, *211*(1), 343-354.
11. Lee S.Y.; Park S. J.; TiO_2 photocatalyst for water treatment applications, *Journal of Industrial and Engineering Chemistry.*, **2013**, *19*(6, 25), 1761-1769.
12. Kormann C.; Bahnemann D.W.; Hoffmann M.R.; Preparation and Characterization of Quantum-Size Titanium Dioxide, *J. Phys. Chem.*, **1988**, *92,* 5196.
13. Goswami D.Y.; A review of engineering developments of aqueous phase solar photocatalytic detoxification and disinfection processes, *J. Sol. Energy.*, **1997**, *119,* 101.
14. Kumar K.J.; Raju N.R.C.; Subrahmanyam A.; Thickness dependent physical and photo catalytic properties of ITO thin films prepared by reactive DC magnetron sputtering, *Applied Surface Science.,* **2011**, *257,* 3075.
15. Chung Y. W.; Yuan L. L.; Yu S. L.; Chen J. L.; Chien H. W.; Thickness-dependent photocatalytic performance of nanocrystalline TiO_2 thin films prepared by sol–gel spin coating. *Applied Surface Science.*, **2013**, *280* 737.
16. Gaya UI.; Abdullah AH. Heterogeneous photocatalytic degradation of organic contaminants over titanium dioxide: A-Review of fundamentals, progress and problems. *J Photochem. Photobiol.*, **2008**, *9*,1.
17. Chen C.; Li X.; Ma W.; Zhao J.; Hidaka H.; Serpone N.; Effect of transition metal ions on the TiO_2-assisted photodegradation of dyes under visible irradiation: a probe for the interfacial electron transfer process and reaction mechanism, *J. Phys. Chem.* B., **2002,** *106,* 318.
18. Ko S., Photochemical synthesis and photocatalytic activity in simulated solar light of nanosized Ag doped TiO_2 nanoparticle composite. Composites: Part B., **2010,** doi:10.1016/j. composites B, 2010.09.007.
19. Rosseler O.; Shankar M.V.; Dum K.L.; Schmidlin L.; Keller N.; Keller V.; Solar light photocatalytic hydrogen production from water over Pt and Au/TiO_2 (anatase/rutile) photocatalysts: influence of noble metal and porogen promotion. *J. Catal.*, **2010**, *269,* 179.
20. Khan R.; Kim T-J. Preparation and application of visible-light-responsive Ni-doped and SnO_2-coupled TiO_2 nanocompositephotocatalysts, *J. Hazard Mater.*, **2009**, *163,* 1179.

21. Hilal H.S.; Majjad L.Z.; Zaatar N.; El-Hamouz A.; Dye-effect in TiO_2 catalyzed contaminant photo-degradation: sensitization vs. charge-transfer formalism, *Solid State Sciences.*, **2007**, *9,* 9.
22. Thompson T.L.; Yates J. J.; Surface science studies of the photoactivation of TiO_2-new photochemical processes, *Chem. Rev.,* **2006**, *106*(10), 4428.
23. Fujishima A.; Zhang X.; Tryk D.A.; TiO_2 photocatalysis and related surface phenomena. *Surf. Sci. Rep.*, **2008**, *63,* 515.
24. Kim S.; Hwang S.; Choi W.; Visible light active platinum-ion-doped TiO_2 photocatalyst, *J. Phys. Chem.* B., **2005**, *109,* 24260.
25. Aprile C.; Corma A.; García H.; Enhancement of the photocatalytic activity of TiO_2 through spatial structuring and particle size control: from subnanometric to submillimetric length scale, *Phys. Chem.*, **2008**, *10,* 769.
26. Sharma V. K.; Yngard R. A.; Lin Y.; Silver nanoparticles: green synthesis and their antimicrobial activities. *Adv. Colloid Interface Sci.*, **2009**, *145*, 83.
27. Liu S.X.; Qu Z.P.; Han X.W.; Sun C.L.; A mechanism for enhanced photocatalytic activity of silver-loaded titanium dioxide, Catal. *Today.,* **2004**, *93,* 877.
28. Jung S. C.; Kim B.H.; Kim S. J.; Imaishi N.; Cho Y.I.; Characterization of a TiO_2 Photocatalyst Film Deposited by CVD and Its Photocatalytic Activity, *Chemical Vapor Deposition.,* **2005,** *11*, 137.
29. Damiriv D.; Bally A. R.; Ballif C.; Homes P.; Schmid P. E.; Sanjines R.; Levy F.; Parvulescu V.I.; Photocatalytic degradation of phenol by TiO_2 thin films prepared by sputtering, *Appl. Catal. B.*, **2000**, *25,* 83.
30. Hoyer P.; Formation of Titanium Dioxide Nanotube Array, Langmuir., **1996**, *12*, 1411.
31. Burnside S.D.; Shklower V.; Barbe C.; Comte P.; Arendse F.; Brookes K.; Grätzel M.; Self-organization of TiO_2 nanoparticles in thin films, *Chem. Mater.*, **1998**, *10*, 2419.
32. Barakat NA.; Kanjwal MA.; Chronakis IS.; Kim HY. Influence of temperature on the photodegradation process using Ag-doped TiO_2 nanostructures: negative impact with the nanofibers. *J Mol Catal A Chem.*, **2013**, *366*, 333-340. Sakthivel S, Shankar MV, Palanichamy M, Arabindoo B.
33. Bahnemann DW.; Murugesan V. Enhancement of photocatalytic activity by metal deposition: characterisation and photonic efficiency of Pt, Au and Pd deposited on TiO_2 catalyst. *Water Res.*, **2004**, *38*(13), 3001-3008.
34. Bensouici F.; Souier T.; Dakhel A A.; Iratni A.; Tala-Ighil R.; Bououdina M. Synthesis, characterization and photocatalytic behavior of Ag doped TiO_2 thin film. *Superlattices Microstruct.*, **2015**, *85*, 255-265.
35. Djerdj I.; Tonejc A. Structural investigations of nanocrystalline TiO_2 samples. *J Alloys Compd.*, **2006**, *413*(1-2), 159-174.
36. Khan M.; Farooq WA.; Saleem M.; Bhatti KA.; Atif M.; Hanif A. Phase change, band gap energy and electrical resistivity of Mg doped TiO_2 multilayer thin films for dye sensitized solar cells applications. *Ceram Int.,* **2019**, *45*(17), 21436-21439.
37. Ao Y.; Xu J.; Fu D.; Yuan C. Preparation of Ag-doped mesoporous titania and its enhanced photocatalytic activity under UV-light irradiation. *J Phys Chem Solid.,* **2008**, *69*(11), 2660-2664.
38. Sakthivel T.; Ashok Kumar K.; Ramanathan R.; Senthilselvan J.; Jagannathan K. Silver doped TiO_2 nano crystallites for dyesensitized solar cell (DSSC) applications. *Mater Res Express.*, **2017**, *4*(12), 126310.
39. Usha K.; Kumbhakar P.; Mondal B. Effect of Ag-doped TiO_2 thin film passive layers on the performance of photo-anodes for dye-sensitized solar cells. *Mater Sci Semicond Process.*, **2016**, *43*, 17-24.
40. Eagen C. Nature of the enhanced optical absorption of dyecoated Ag is land films. *Appl Optics.*, **1981**, *20*(17), 3035-3042.
41. Demirci S.; Dikici T.; Yurddaskal M.; Gultekin S.; Toparli M.; Celik E. Synthesis and characterization of Ag doped TiO_2 heterojunction films and their photocatalytic performances. *Apply Surf Sci.*, **2016**, *390*, 591-601.
42. Li Y.; Ma M.; Chen W.; Li L.; Zen M. Preparation of Ag-doped TiO_2 nanoparticles by a miniemulsion method and their photoactivity visible light illuminations. *Mater Chem Phys.*, **2011**, *129*(1-2), 501 -505.